

Magnetic bearing stages for electron beam lithography

Paul T. Konkola

konkola@mit.edu.

David L. Trumper*

trumper@mit.edu.

Department of Mechanical Engineering, Massachusetts Institute of Technology, Cambridge, MA

1 Abstract

While electromagnetic actuators have been proven in many precision motion control applications, their stray fields constrain their use in systems that require high stability of charged particle beams. Fringing fields from these actuators should be sufficiently small to have minimal influence on the trajectory and focusing properties of the charged beams.

We have built a levitation linear motor that is designed to have significantly reduced fringing fields. The design achieves large far field attenuation because of parallel opposing multipole placement in the synchronous motor bearing. The design is suitable for future generations of electron beam lithography, where the allotted error due to stage fringing fields may be less than 1 nm. The low fringing field design attains very strong fields at the stator, where force is generated, while the fringing fields fall very rapidly. Whereas fields for a dipole fall off as radius⁻³, the paper presents a prototype synchronous motor magnet array with fields that fall off largely as radius⁻¹⁰ in the far field. The stator has fields that fall off as radius⁻⁵.

The novel permanent magnet array and coil array technologies can be implemented in stage designs where the fringing field is designed to have negligible influence on the electron beam in a lithography machine. The stator and magnet array have a sufficiently low field to allow placement of the arrays unusually close to the electron beam. This allows a compact, high resonant frequency stage structure. A precision motion control stage based on the low fringing field magnetic bearing is thus shown to be feasible for next generation electron beam lithography.

*presenter

2 Introduction

Magnetic bearing stages are a promising motion control alternative in electron beam lithography and other high precision charged particle systems [4]. Although an electron beam system has the capability to feedback stage errors to a high bandwidth beam deflector, the structural vibrations of the stage couple with the metrology frame to limit the accuracy of the feedback signal and the consequent placement accuracy. Therefore, stage disturbance sensitivity and disturbance rejection are critical to the performance of state of the art electron beam lithography machines.

Magnetic bearing stages are attractive for many reasons. They can be a mechanically simple yet highly functional design, where a single moving part is controlled in six degrees of freedom [1, 2, 7]. They can achieve large-scale planar motion and small-scale focusing and rotational alignments. A compact, high resonant frequency stage structure is possible with the single moving part design. Additionally, the stage is not limited by precision bearing surfaces, friction, or backlash. Therefore, the positioning performance can be extended to the limits of control and metrology. This translates not only into more precise motion but many difficult disturbance sources that induce substrate and metrology frame vibration are also eliminated. Furthermore, a magnetically suspended part is relatively insensitive to base disturbances because it is not mechanically coupled to the machine base. Thus, magnetic bearing stages have the potential for reduced disturbance sensitivity and better achievable disturbance rejection through control.

Since no lubrication is required, a magnetic bearing stage is highly suited to the vacuum environment. Particle generation is also lowered since the suspended stage does not generate wear particles. Addi-

tionally, stringent thermal stability requirements for the substrate and metrology frame is possible since there is no heat dissipation on the moving part and there is large thermal resistance between the part and the power dissipating components.

From the system-level perspective, magnetic bearing stages have the potential for additional benefits. A single moving part is a highly reliable mechanical system, thereby improving the machine up-time and maintainability. Additionally, the cabling to the moving part is minimal – perhaps consisting of only a ground lead. Thus, this disturbance source is largely removed. There is also the potential for a smaller stage footprint, thereby reducing the size of the vacuum chamber. This leads to lower loads on the vacuum system, less demand on chamber shielding, better column-to-chamber structural properties, and in general a less expensive and higher performance system. Furthermore, the small chamber should experience less vibration disturbances from the lower capacity vacuum machinery and from acoustic air vibrations.

However, a stage suitable for ebeam lithography must be carefully designed to meet the requirements for electron beam placement accuracy. In the best case, the stage would have no influence on the electron beam trajectory and the focusing properties. However, this need not be the case if the deflections are repeatable with stage position and control effort; an error signal could be used to drive the electron beam deflector. This requires a way to calibrate these errors. Because achieving high calibration accuracy is difficult, especially for short spatial period errors, there is a limit to how much beam correction can be allowed.

The goal of this work is to prove the feasibility of magnetic bearings for electron beam lithography by showing they can have an insignificant influence on the electron beam trajectory when placed at reasonable distances (electron beam ≈ 15 cm from magnets or coils). These low fringing field bearings will allow smaller, high resonant frequency stages than would otherwise be possible.

Our calculated requirement for a stage fringing field crossing the electron beam at the write plane is $< 2 \times 10^{-7}$ T for an allowance of 1 nm of deflection error [4]. This calculation assumes a 50 kV electron beam, a 3 mm unshielded beam length, and assumptions about the column shielding and objective lens properties.

3 Synchronous motor bearings for low fringing fields

Low fringing field magnetic bearing design may include a combination of techniques including

- large spacing requirements between the magnetic components and the location where large attenuation is desired
- shielding
- field cancellation

Since the high resonant frequency stage designs of interest for future generations of electron beam lithography require a small footprint, large spacing is not an option. Also, large spacing requires a heavier stage structure and stronger actuators to support it. The option of shielding can play a limited role in magnetic bearing for electron beam lithography. Moreover, the low fringing field requirement will not likely be met if moving iron is in the writing chamber. Similarly, moving permeable material in the presence of externally supplied field will distort the magnetic field as it moves through it. This field will cause deflections of the electron beam. Large fields ($> 10^{-4}$ T) exist in the chamber due to the strong objective lens, which is necessary to finely focus the electron beam. Although shielding topologies [4] exist where there is no moving iron, they unfortunately require a big, heavy stage structure. For our work, we have pursued field cancellation as the solution to low fringing field magnetic bearing design.

We have focused on synchronous motors for this application because all the following properties can be met

- forces in multiple directions can be precisely controlled
- opposing dipoles are inherent in the design and allow field cancellation topologies
- rare earth magnets have strong intrinsic magnetization and no hysteresis during normal use
- rare earth magnets and copper coils very closely approximate the permeability of free space
- force output of low permeability material based motor designs are relatively insensitive to the size of the "air" gap

- synchronous motors have been proven in precision motion control systems for six degree of freedom positioning [1, 2, 7].

We have designed and built a low fringing field magnetic bearing based on field cancellation designed into a planar synchronous motor.

4 Experimental implementation

Figure 1 shows the experimental apparatus to test the magnetic field and force properties of the prototype synchronous motor. This apparatus is also shown as a schematic in Figure 2. The major subassemblies include a magnet array, stator, laser interferometry system, force sensor system, air bearing, and support structure. The magnet array and stator form a synchronous motor that produces independently controllable forces in suspension and translation.

The magnet array and stator are low fringing field designs that implement field cancellation techniques that we developed. The laser interferometry system and the force sensor system is used to assess the electromechanical performance of the synchronous motor bearing. Also, the setup is a test bed for precision motion control experiments. The travel is over 33 cm. Although the air bearing constrains the motion to a single translation degree of freedom, the full electromechanical performance of the synchronous motor can be assessed because the force sensors transduce the suspension force; three piezo force sensors support the air bearing rod and the sum of the charge output from them indicates the suspension force. The moving mass was designed to represent approximately one fourth the mass for a light weighted stage that would require 33 cm \times 33 cm of travel. The prototype moving mass is 5.2 kg. Also, for field measurements a flux gate magnetometer (Bartington Mag-03MC100 three axis flux gate magnetometer) is employed. The experiments lead to the characterization of the fields and the electromechanical performance of the magnetic bearing.

A schematic of the prototype magnet array is shown in Figure 3. It is a variation of a block Halbach array that takes advantage of field cancellation produced by parallel opposing dipoles.

The array is built from magnets with 0.64 cm \times 0.64 cm cross section. All magnets have the same nominal remanence. The overall width of the array

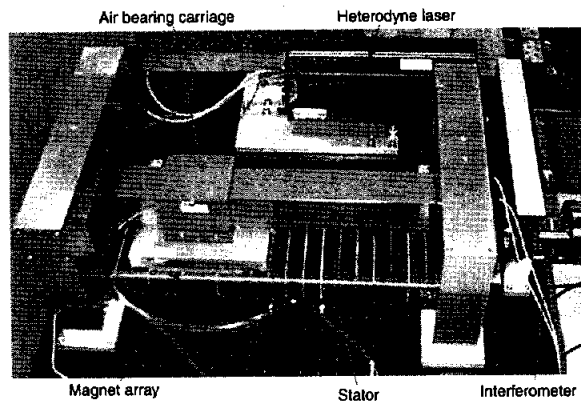


Figure 1: Experimental apparatus.

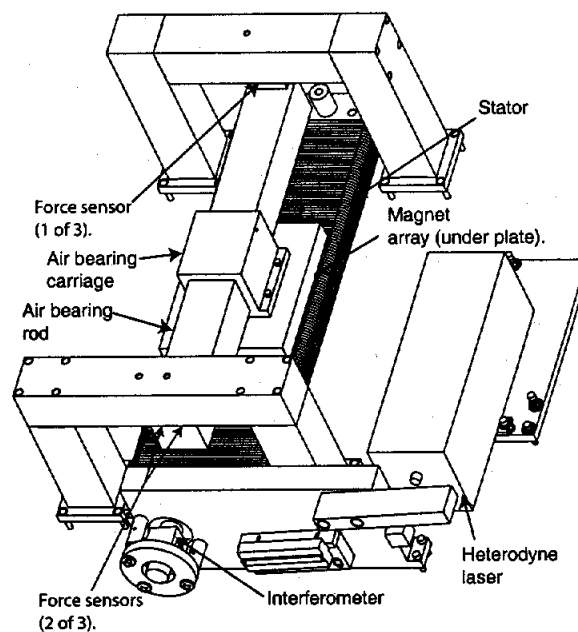


Figure 2: Schematic of the experimental apparatus.

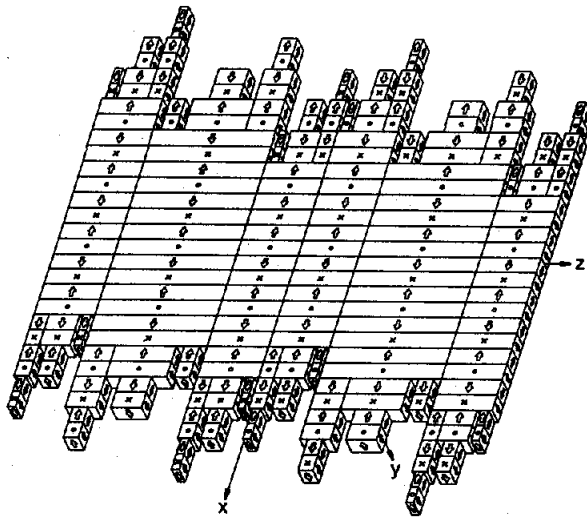


Figure 3: Prototype magnet array. All magnets have the same remanence. Arrows point to the north pole of each magnet.

is 17 cm. Only five magnet versions, where only the length varies, are used to build this array.

The prototype magnet array is constructed from parallel opposing dipoles – a single magnet closely approximates a dipole in the far field. The dipoles are arranged such that seven levels of cancellation superpositions are achieved. Based on a scheme for arranging the magnet arrays in parallel opposing configurations, sub-arrays are superposed to create higher order multipoles. Each superposition is based on dividing the previous multipole array into smaller, opposing multipoles. For instance, given a magnet array, a higher order multipole with the same magnet area is created by attaching an array with half the product of the dipole moment and the multipole moment arms to an identical array but with magnetization of the reverse sign. For a synchronous motor, the arrays need to be attached such that the magnetization of the arrays maintains constant rotation of the magnetization. Therefore, the opposing arrays are offset by half a spatial period. For the prototype, the scheme for arranging the magnet arrays above the second superposition also results in a multipole moment arm with a sideways offset. The sideways offset results in the magnetic “fingers” visible in the figure. The details of the design procedure for this array and others can be found in [3, 4]. Other designs based on a more efficient cancellation scheme are also discussed

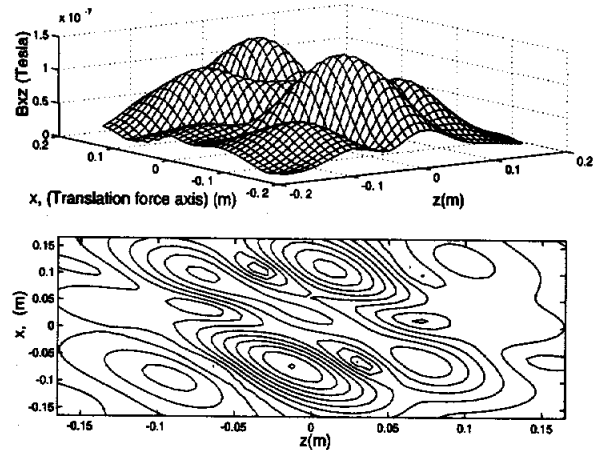


Figure 4: The top plot shows B_{xz} at $y = -0.15$ m above the prototype magnet array center plane. The maximum value is 1.49×10^{-7} T. Below is the contour plot of the same data. The minimum contour is 8.24×10^{-9} T. The maximum contour is 1.48×10^{-7} T.

in those references. The prototype topology was chosen mainly for manufacturing reasons; it requires relatively few versions of magnets and all the magnets have the same remanence.

The required area of magnets for a given application can be estimated from a two dimensional analysis given the required force, the magnet array properties (spatial period, magnet height, remanence), and other factors including the range of gap and the thermal current limit. The experimental force output of the motor was measure to be 88% of that calculated using a two dimensional analysis detailed in [6].

Figure 4 shows the theoretical magnetic flux density 0.15 m above the magnet array center plane. The calculations were performed using magnetic charge integration [4, 5]. The flux density, B_{xz} , is the magnitude of the magnetic field that would cross the ebeam path where $B_{xz} = \sqrt{B_x^2 + B_z^2}$. The coordinate system is shown in Figure 3 and its origin is located at the array centroid. The maximum flux density is 1.49×10^{-7} T. While the range of fields affecting the ebeam depends on the placement of the array on the moving part and the travel, the flux density shown represents the worst possible range with this array. In a real application, the array is likely to be displaced laterally relative to the e-beam and fields outside the plotted $x - z$ range drop further.

Figure 5 shows the theoretical magnetic flux density 0.15 m above a conventional quadrupole synchro-

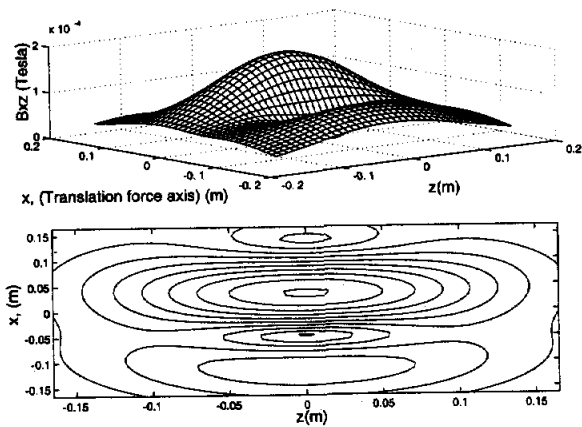
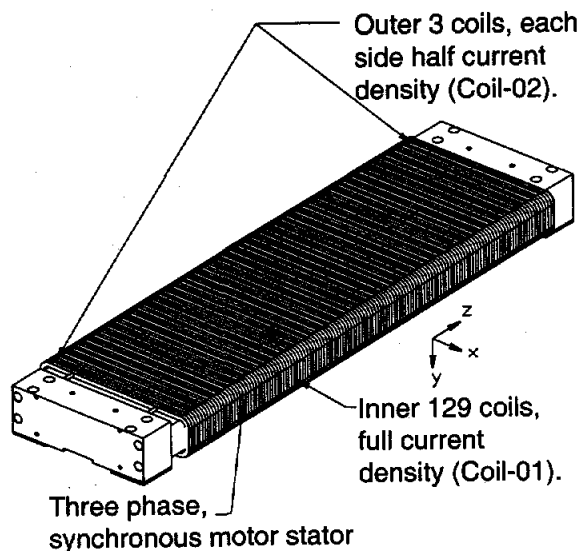


Figure 5: The top plot shows B_{zz} at $y = -0.15$ m above a conventional quadrupole synchronous motor with approximately the same force constant as the prototype array. The maximum value is 1.85×10^{-4} T. Below is the contour plot of the same data. The minimum contour is 1.26×10^{-5} T. The maximum contour is 1.83×10^{-4} T.

nous motor magnet array. The array has the same area in the $x - z$ plane as the prototype array and approximately the same force constant. A synchronous motor with an integer number of periods has fields that fall off like a quadrupole where the field decays as radius⁻⁴ in the far field. The calculations again were performed using magnetic charge integration. The maximum flux density is 1.85×10^{-4} T, which is over 1200 times that of the theoretical result for the prototype array.

The experimentally measured magnetic fields from the prototype array do not achieve the theoretical performance. We expect this is due to tolerances in the magnets and in their assembly. This property was predicted with Monte Carlo simulation. The measured fields of the magnet array indicate fields of less than 2×10^{-7} T at 41 cm from the array. Whereas theory predicts fields dropping to this level by only 15 cm separation, this much larger separation is due to magnetization and assembly tolerances. Our Monte Carlo simulation predicted this field at about 46 cm from the array assuming remanence variations in the magnets of $\pm 3\%$, angular variations of magnetization density vectors of $\pm 3^\circ$, and magnet placement tolerances of ± 0.3 mm. It was found that both the angular variation and remanence variations are especially detrimental to the performance of the array. The angular and remanence tolerances were the best avail-



Coil Cross Sections

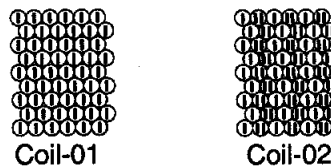


Figure 6: Prototype stator. The top view shows the stator assembly. It consists of 135 coils wired to form a three phase synchronous motor. Of these, 129 are full current density coils. The outer 3 coils on each end are half current density coils with the bifilar winding as shown for Coil-02.

able to us in the limited time of this project. A single magnet with volume equal to 0.051 cm^3 placed at the center of the array would produce a field of the measured strength. This represents 0.04% of the array volume. Considering this sensitivity to magnet and assembly tolerances, a practical array must be manufactured with compensation schemes. Further design and the placement of additional trimming magnets will improve the performance to approach that of the theoretical array.

Our prototype stator is shown in Figure 6. The stator consists of 129 full current-density coils and 3 half current-density coils on each end. The coil cross sections are shown in the figure. The full current density coil is wound with a single wire. The half current density coils have a bifilar winding. Connecting both wires in parallel produces half the current den-

sity when wired in series with the full current density coils.

This stator can be modeled as a multipole with fields that decay as radius⁻⁵ in the far field. There are two levels of cancellation beyond a dipole. The first level of cancellation is due to the opposing dipoles inherent in a conventional synchronous motor stator with an integer number of spatial periods. For this three phase stator, one spatial period consists of 6 coils. The outer cross sectional dimension of a coil is 19 cm in the x direction, 4.8 cm in the y direction, and 0.42 cm in the z direction. The overall length of the coil stack in the z direction is 52 cm.

Figure 7 shows the theoretical magnetic flux density 0.15 m above the stator array center plane. The calculations were performed using the same algorithm as for the magnet arrays by substituting magnetic charge for equivalent surface currents.

The coordinate system orientation is in Figure 6 and its origin is located at the coil stack's centroid. The maximum flux density is 7.6×10^{-8} T. Again the range of fields affecting the ebeam depends on the placement with respect to the ebeam. The flux density shown represents the fields when the stator is nominally centered beneath the ebeam. Commutation of the currents during stage travel essentially changes the field orientation. These fields will rotate through a change of 180° whenever the stage moves through half the synchronous motor spatial period.

Figure 8 shows the theoretical magnetic flux density 0.15 m above a conventional quadrupole stator. This stator consists of 132 full current density coils. The maximum flux density is 4.8×10^{-7} T, which is greater than 6 times that of the theoretical prototype array. The relatively low surface currents in the stator compared to the equivalent surface currents in the rare earth magnets makes the required cancellation performance a less demanding task.

Experimental field data from the stator is shown in Figure 9, where the distance $\text{abs}(y)$ is in the negative y direction as per the coordinate system shown in Figure 6. The theoretical data contains a small correction where field contributions due to the coil leads are included. The experimental data was taken with the magnetometer probe over approximately the middle of the coil stack. The nominal current is 0.4 amps. The absolute position of the magnetometer was known to about ± 3 mm in this setup. Theoretical and experimental data is shown for current flowing in each of the three phases. At the distances of interest the experimental data corresponds well with

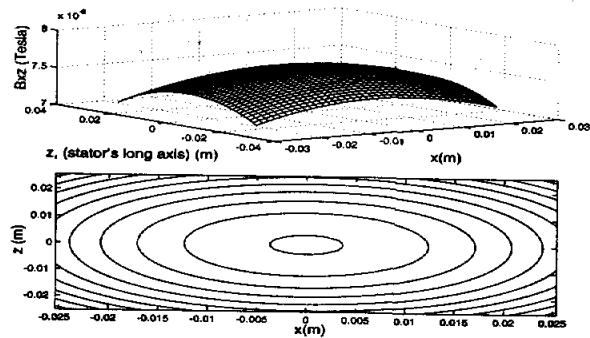


Figure 7: The top plot shows B_{zz} at $y = -0.15$ m above the stator center plane. The maximum value is 7.6×10^{-8} T. Below is the contour plot of the same data. The minimum contour is 7.1×10^{-8} T. The maximum contour is 7.6×10^{-8} T. The current is set to the value required to suspend the prototype mass ($F_y = -51$ N).

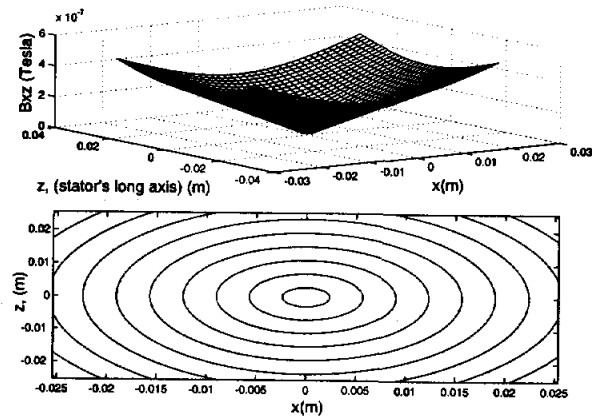


Figure 8: The top plot shows B_{zz} at $y = -0.15$ m above a conventional quadrupole stator. The maximum value is 4.8×10^{-7} T. Below is the contour plot of the same data. The minimum contour is 3.6×10^{-8} T. The maximum contour is 4.8×10^{-7} T. The current is set to the value required to suspend the prototype mass ($F_y = -51$ N).

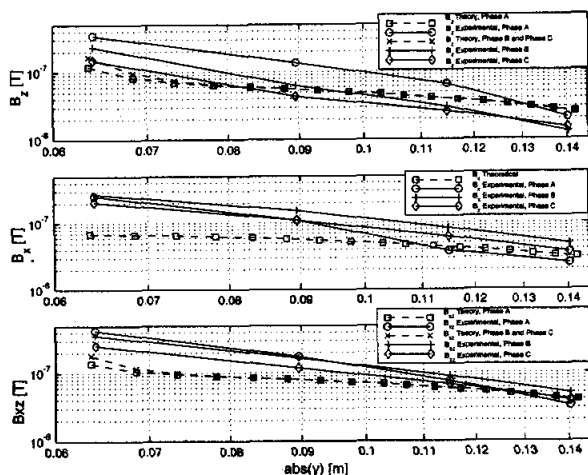


Figure 9: Experimental and theoretical data for magnetic flux density measured above the mid point of the stator.

the theoretical.

5 Conclusions

We have shown that synchronous motors can be designed with significantly reduced fringing fields. The magnet array design achieves a theoretical fringing field of a less than 2×10^{-7} T at a distance of about 15 cm above the magnet array surface. A "conventional" quadrupole synchronous motor array with the same force capability would achieve 2×10^{-7} T at about a 91 cm spacing. At 15 cm of spacing the quadrupole synchronous motor would have fields over 1200 times larger than the low fringing field design. The measured magnetic fields from the prototype array do not achieve the theoretical performance because of tolerances in the magnets and in their assembly. This property was predicted with a Monte Carlo simulation. The measured fields of the magnet array indicate fields of less than 2×10^{-7} T at 41 cm from the array. Monte Carlo simulation predicted this field at about 46 cm assuming the specified tolerances of the magnets and the assembly. A single magnet that is 0.04% of the array volume would produce the measured field. Considering this sensitivity to magnet and assembly tolerances, the array must be manufactured with additional trimming magnets. The prototype stator achieves a fringing field of a less than 1×10^{-7} T at a distance of about 13 cm above the stator surface when supporting the magnet ar-

ray with a 51N suspension force. The calculated and measured stator fringing fields have good correspondence. A precision motion control stage based on our low fringing field magnetic bearing techniques is thus shown to be feasible for next generation electron beam lithography.

References

- [1] Michael Holmes. *Long-Range Scanning Stage*. PhD dissertation, UNC-Charlotte, Department of Electrical Engineering, June 1998.
- [2] Won jong Kim. *Planar Magnetic Levitation*. PhD dissertation, Massachusetts Institute of Technology, Department of Electrical Engineering and Computer Science, June 1997.
- [3] Paul Konkola and David L. Trumper. Methods and apparatus involving selectively tailored electromagnetic fields. *United States Patent 6,316,849 B1*, 2001.
- [4] Paul Thomas Konkola. Magnetic bearing stages for electron beam lithography. Master's thesis, Massachusetts Institute of Technology, Department of Mechanical Engineering, February 1998.
- [5] R. D. Schlueter and S. Marks. Three dimensional pure permanent magnet undulator design. *IEEE Transactions on Magnetics*, 32(4):2710+, July 1996.
- [6] David L. Trumper, Mark E. Williams, and Tiep H. Nguyen. Magnet arrays for synchronous machines. *Proceedings of the IEEE IAS 28th Annual Meeting*, pages 216–223, October 1993.
- [7] Mark E. Williams. *Precision Six Degree of Freedom Magnetically-Levitated Photolithography Stage*. PhD dissertation, Massachusetts Institute of Technology, Department of Mechanical Engineering, February 1998.

